Unsteady conjugate heat transfer analysis for impinging jet cooling

F Tejero, P Flaszyński, R Szwaba and J Telega
The Szewalski Institute of Fluid-Flow Machinery (IMP PAN),
Fiszera 14, 80-231 Gdańsk, Poland

E-mail: fernando.tejero@imp.gda.pl

Abstract. The paper presents the numerical investigations of the heat transfer on a flat plate cooled by a single impinging jet. The thermal conductivity of the plate was modified from a high thermal case (steel - λ = 35 W/m/K) to a low one (steel alloy Inconel - λ = 9.8 W/m/K). The numerical simulations results are compared with the experimental data from the Institute of Fluid-Flow Machinery Polish Academy of Sciences, Gdansk (Poland). The numerical simulations are carried out by means of Ansys/Fluent and k-ω SST turbulence model and the temperature evolution on the target plate is investigated by conjugated heat transfer computations.

1. Introduction

Heat transfer and cooling effectiveness of impinging jets application is being investigated by several researchers recently. It was during the 50s when Freidman and Mueller [1] reported the first research conducted on this topic. Among other purposes, there has been a big effort on turbine cooling applications [2,3] where the impinging jets might cool several sections of the engine such as the combustor, the turbine case and/or the turbine blades. The effects of a crossflow in a jet array impingement on the heat transfer was investigated by Flourscheutz et al. [4]. The research of the use of the liquid crystal technique to study the local heat transfer coefficient was carried out by Metzger and Bunker [5] and it is employed in the present investigation as well.

The proper design of an impinging jet is challenging due to the large number of parameters which should be considered and play an important role in the heat transfer effectiveness. During last years, there have been several investigations such as the studies of the effect of the jet-hole size and distribution, target surface shape (bumps configuration) or cooling channel cross-section.

The influence of plate material (change of the thermal conductivity, λ) on the heat transfer by impinging jets is investigated in the present paper. Two different material properties were studied for a plate thickness of 2 mm. The thermal conductivity of the plate was modified from a high thermal case (steel - λ = 35 W/m/K) to a low one (steel alloy Inconel - λ = 9.8 W/m/K). The unsteady simulations allowed for a better understanding of the flow physics when an impinging jet is applied. Besides, the temperature evolution on the investigated plate is successfully compared with the available experimental data (Transient Liquid Crystal measurements).

It is expected that the heat transfer efficiency might be improved by the use of rough plates (this paper presents only the smooth plate configuration). The final objective of the Innolot-Coopernik project investigations is to study the impact of different type of roughness (structured and/or unstructured) on the thermal effect of the applied impinging jet. Nevertheless, the numerical results

presented here are very important for validation of the CFD and measurement techniques as first step for more complex configurations.

2. Experimental setup

In Figure 1, a sketch of the test section employed during the experiments is presented. The distance between the impinging jet nozzle outlet and the plate was modified from 4mm to 7mm (CFD results presented below are for the 4mm configuration). To avoid conduction between ambient and the side of the plate that is not interacting with the jet, it was isolated by a thick PMMA plate of low thermal conductivity ($\lambda = 0.21$ W/m/K).

The camera employed was the 3CCD JAY CV-M9GE which is capable of taking 30fps films with 24 bit color depth (8 bits for each of the RGB components). The plate is thermally isolated from its holder by PTFE elements. Once the plate is fixed, it can be precisely adjusted with micrometric screws along the flow direction. In order to control the activation of the impinging jet, a thermal shield was machined of 3mm thick plywood. If it is set in the "inactive" position, the shield covers the plate, isolating it from the oncoming flow (no influence of the jet on the plate temperature can be noticed). On the other hand, if the shield is removed, the interaction of impinging jet and plate starts.

The cylindrical nozzle of 2mm diameter and a hot air soldering station PT852 has been adapted to supply the air for the jet. Mass flow rate control is realized by an ALICAT flowmeter. The temperature is measured by a four K type thermocouples. Every temperature measurement channel has been calibrated using the DRUCK DBC150 Temperature Calibrator with 0.7ºC absolute precision. The calibration function (mapping the measured temperature to real temperature) has been calculated by means of linear regression. This has been done for every thermocouple, and the coefficients have been implemented in the measurement software.

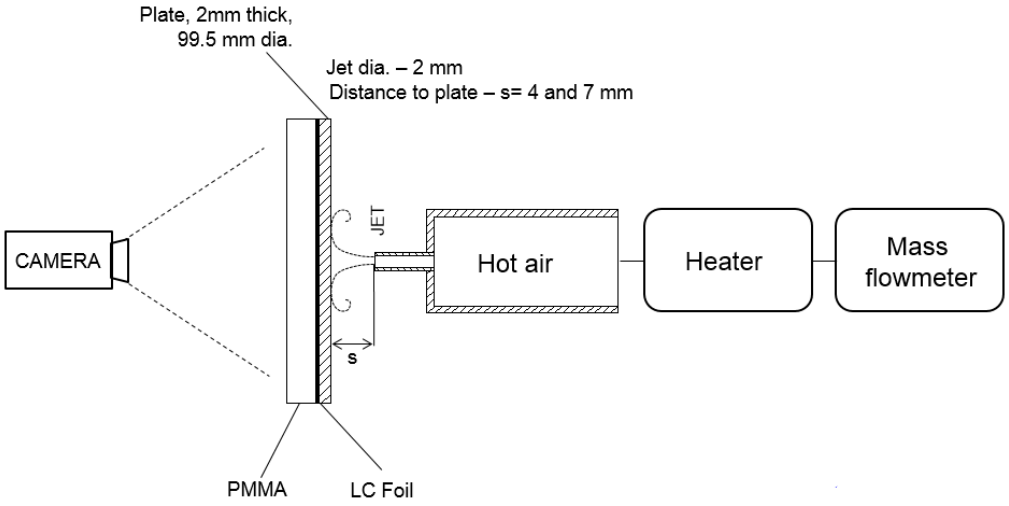

Figure 1. Sketch of the experimental setup

The investigated plate 2mm thickness and 99.5mm diameter are made of steel. One side of the plate is covered with TLC (Thermochromic Liquid Crystal) adhesive foil, while the hot air jet impinges the other side. Figure 2 presents both sides of the steel plates investigated. The red frame indicates the thermocouple wiring for plate temperature evolution in the experiment. The thermocouple sensor was located in the plate center and in the middle of plate thickness.

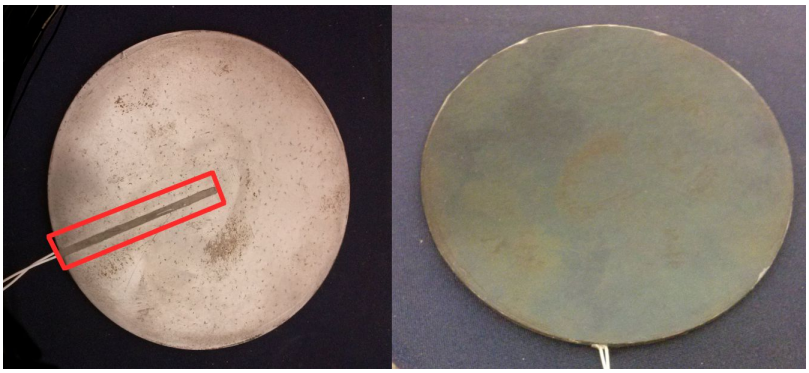

Figure 2. Investigated steel plates

3. CFD investigation

3.1. Numerical method

The numerical investigations were carried out by means of the Ansys/Fluent code which solves the Unsteady Reynolds-Averaged Navier-Stokes (URANS) equations with various turbulence models. From the different turbulent closures available, the two equation k-ω SST was chosen. The system of differential equations was closed by a perfect was model and the viscosity value was calculated according to the Sutherland´s law. The numerical algorithm was based on a semi-discrete approach with finite-volume of 2nd order of accuracy for the spatial discretization as well as a 2nd order for the time-stepping scheme. The CFL number was set to 20 with the under-relaxation factor of density, body forces, turbulent kinetic energy, specific dissipation rate, turbulent viscosity and energy equal to 0.5. The unsteady simulations were performed in two stages: 1000 times steps with Δt = 5e-5s at the beginning of the computation to develop the flow in the domain and then the time step size was increased to Δt = 5e-4s for the remaining time of the simulation. It is important to mention that due to the large number of time steps needed (flow during more than 50 s is simulated which means more than 100,000 time steps), the computational domain was simplified to an axisymmetric approach, reducing considerably the number of volumes and the computational resources. The independence of the solution on the time resolution was successfully proven by the time step reduction by a factor of ten, in both stages of the simulations (i.e. Δt = 5e-6s for the first step 1000 iterations and Δt = 5e-5s for the second step of the simulation).

3.2. Computational domain – grid topology and boundary conditions

The computational domain of the impinging jet configuration is divided into 15 structured blocks (see Figure 3). The grid is generated semi-automatically using parameterized python scripts within the IGG (Numeca) software. In order to ensure a proper prediction of the boundary layer, the distance of the first grid point from the solid walls (steel and PMMA plates) is of the order if y^+ = 1. The proposed grid has approximately 40,000 cells. This low number of mesh cells is caused by the implementation of the axisymmetric approach in the numerical model. The number would grow up to 2,000,000 volumes for a fully 3d approach, which it is still acceptable, but due to the large number of time steps needed in the simulations, the reduction of the domain was applied.

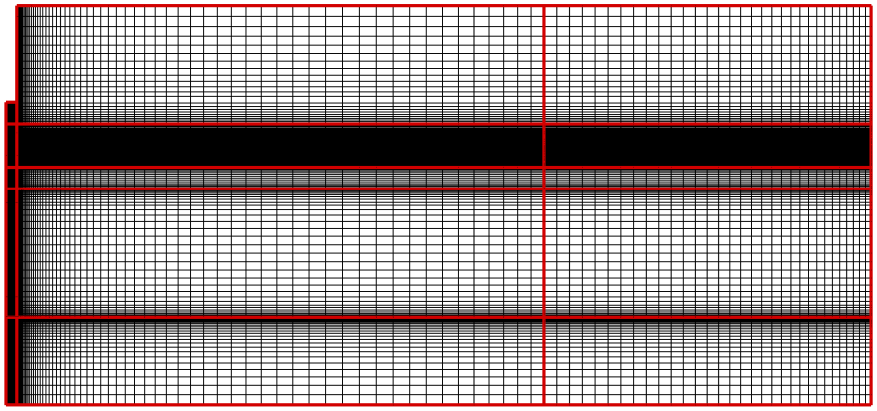

Figure 3. Structured grid and topology of the test section

The computational domain is closed by boundary conditions of 4 types: viscous and inviscid wall, mass flow inlet and pressure outlet (see Figure 4). Table 1 summarizes the conditions at the inlet and outlet of the domain. The outlet of the domain was set 30mm away in radial direction from the investigated plate (more than 30% of its diameter) which is proved to have no influence on the flow field in the near by the plate. On the other hand, the distance from the plate to the upper inviscid wall of the domain was set to 15mm (more than 7 times the thickness of the plate). It was observed how the interaction jet-surface created a wake which influenced the temperature propagation at the plane when the distance to the upper wall was not large enough. The faces of the domain colored by light blue and yellow were considered as solid (conjugated heat transfer is studied) and the heat conductivity of the materials were applied in the numerical model.

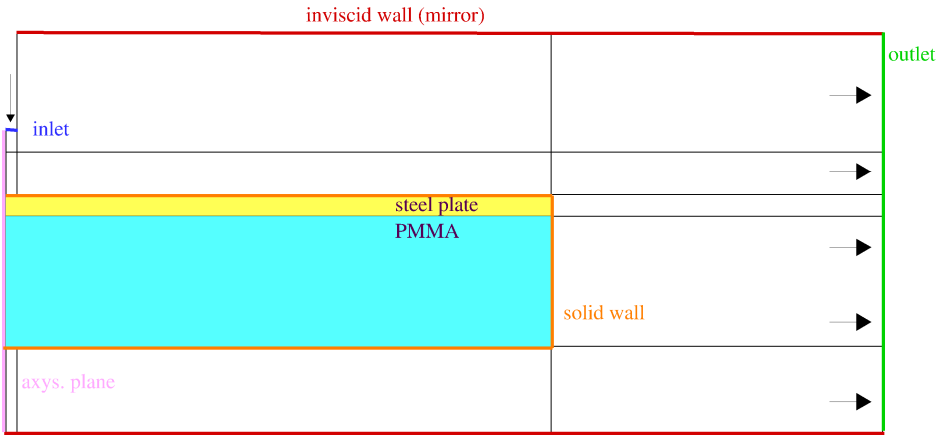

Figure 4. Boundary conditions of the numerical model

Table 1. Inlet and outlet boundary conditions

mass flow inlet	pressure outlet
Mass flow rate [kg/s]: 2.2e-4	Gauge pressure [Pa]: 101000
Turbulent intensity [%]: 0.5	Turbulent intensity [%]: 0.5
Turbulent viscosity ratio [-]: 10	Turbulent viscosity ratio [-]: 10
Total temperature [K]: 363	Total temperature [K]: 293

3.3. Numerical results for the single impinging jet

When a hot jet impinges on the plate, certain time is needed to propagate the temperature in radial direction. There are several parameters which determine the heat transfer speed such as: mass flow of the hot jet, distance jet/surface or temperature of the jet. In the present simulations, the full domain (fluid and solid) are initialized with the reference temperature of 293K. After certain time, the temperature starts to develop and the influence of the heat conduction of the target plate can be investigated. Figure 5 present three snapshots of the temperature contour map (t = 0.05, 20 and 40 s.) for the low conductivity case (λ = 9.8 W/m/K). At the beginning of the simulation (t = 0.05 s) the jet impacts the target surface and its influence is weakly visible. After certain time (e.g. t = 20s), the influence of the hot jet in all the domain is visible: above the plate, the fluid is heated with a propagation of the heat in radial direction inside the steel plate and with a small penetration in the PMMA. If the hot jet continues interaction with the target surface (t = 40s), the heat propagates in radial direction of the plate and penetrates more into the isolating material (PMMA).

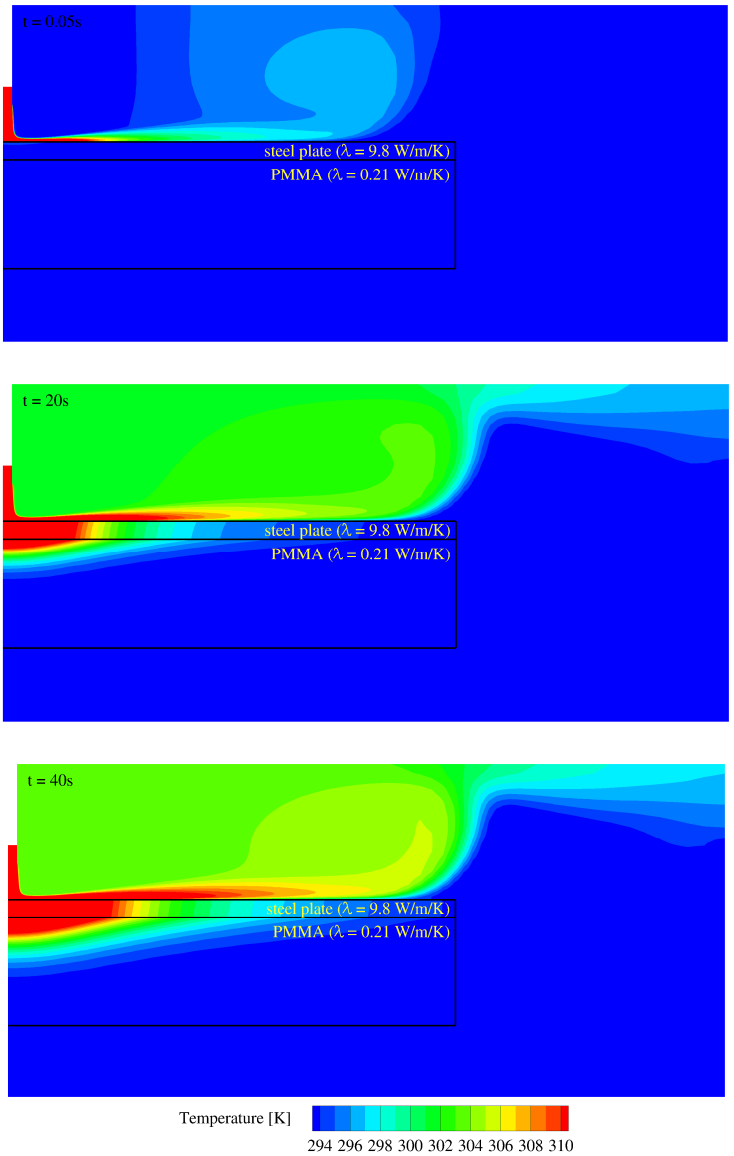

Figure 5. Temperature evolution of the low thermal conductivity case (λ = 9.8 W/m/K)

Figure 6 presents three snapshots of the temperature evolution for the high conductivity case (λ = 35 W/m/K). Since the time response for heating the plate is higher than 0.05s in both configurations investigated, no differences can be found in the first picture of Figures 5 and 6. After certain time, the heat starts to develop in radial direction of the target plate (see Figure 6, t = 20s). Although the thermal conductivity is higher in this case, it is required more time to propagate the heat in the plate. Finally, the last snapshot (t = 40s) shows how the conduction of the heat is still ongoing but also slower than for the low conductivity configuration.

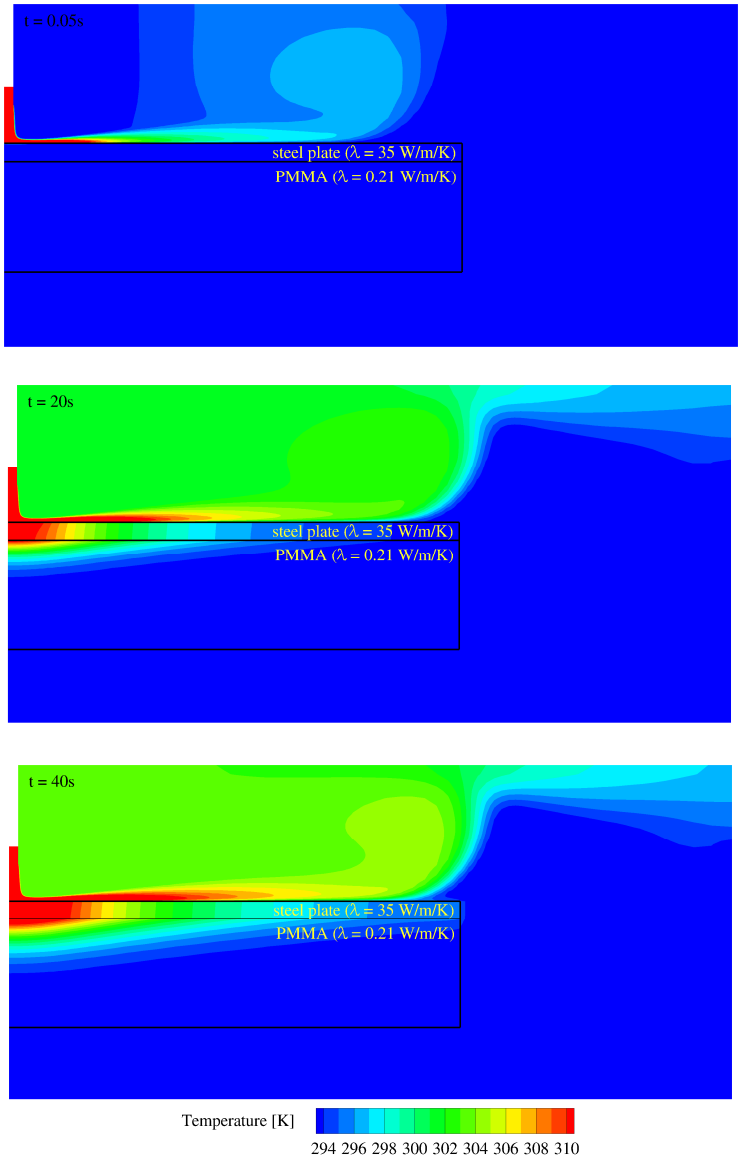

Figure 6. Temperature evolution of the low thermal conductivity case (λ = 35 W/m/K)

During the measurements, the temperature value of 308 K was chosen as reference and its propagation in the radial direction of the steel plate was tracked. Figure 6 presents the comparison of the temperature evolution in radial direction for two cases: high conductivity (λ = 35 W/m/K) and low conductivity (λ = 9.8 W/m/K). In the case of the low conductivity case, the time response of the investigated plate to heat up until the reference temperature near the stagnation point is well reproduced by CFD (approximately t = 2 s). With increased time, the target temperature moves in radial direction. Although, it is visible how the propagation is faster in the experiments than in the CFD, the slope in both investigations remains the same. In the high conductivity case, the response time for the propagation next to the stagnation point is satisfactory reproduced by the numerical simulations (approximately t = 9 s). Overall, it is visible how the CFD simulations presents a quicker propagation of the heat in the plate than the measurements. The differences arises from the change of slope caused, possibly, by the uncertainty of the exact value of the heat conductivity used during the experiments. It is also important to remark that the uncertainty of the measurements (0.7 ºC) might influence the slope of the curve for high conductivity materials (due to the slow changes of the temperature in radial direction).

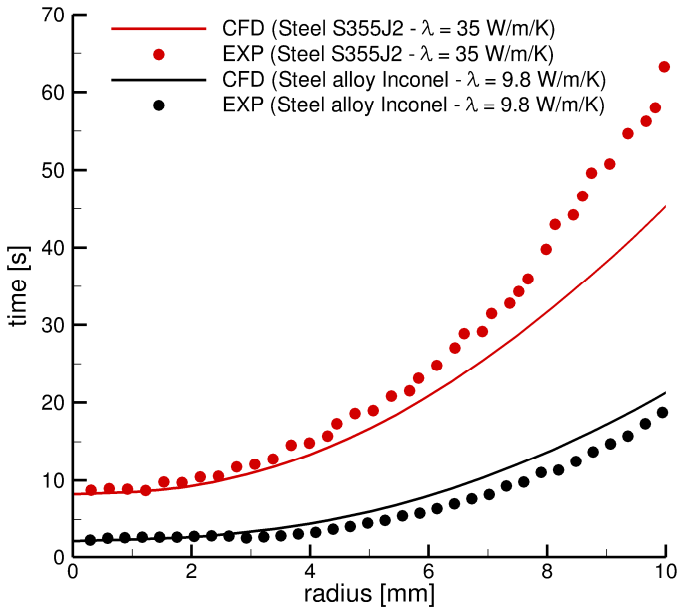

Figure 7. Comparison of the temperature propagation (T = 308K) in radial direction in the steel plate

Figure 8 presents a sensitivity investigation of the influence of the thermal conductivity on the radial propagation of a fixed temperature (308 K). It is shown how the time required to achieve the temperature threshold at the bottom side of the plate is shorter for low conductivity plates. Besides, if the certain temperature is reached close to the stagnation point, the evolution in radial direction is faster (shown by "flat" part of the curves). On the other hand, the flat behavior is followed by a curve of certain slope, which increases for higher conductivity cases.

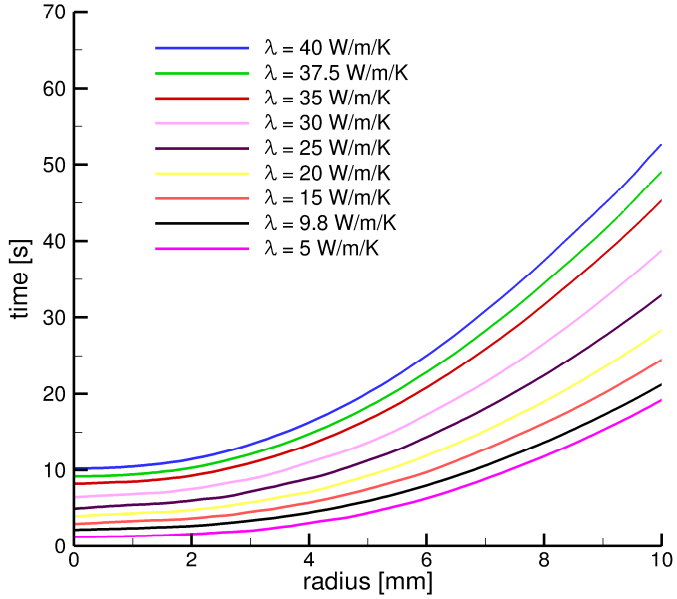

Figure 8. Sensitivity investigation of the plate thermal conductivity

Investigations of the surface modification effect on heat transfer can be assessed by heat transfer coefficient (HTC) comparison. In case of investigated configuration and applied Transient Liquid Crystal Technique, the influence of the conductivity and time dependence is an important feature. In Figure 9, the instantaneous pictures of heat transfer coefficient distribution in radial direction for investigated plates are shown. The HTC is comparable for both plates of different conductivity. Although the plates are heated up in time (as showed above), the HTC remains weakly dependent on time.

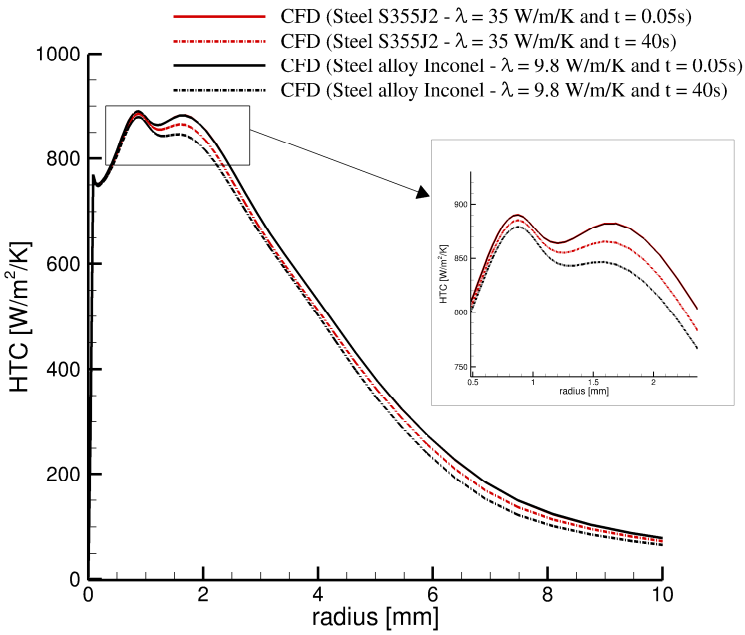

Figure 9. Comparison of heat transfer coefficient

4. Conclusions

The paper presents the details of the numerical simulations of heat transfer by a single impinging jet on a target surface. The effects on the thermal conductivity of the plate were successfully investigated. Numerical results and experimental data have satisfactory agreement for both configurations considered: low and high conductivity. The time needed to heat a plate to certain temperature and its evolution in radial direction was investigated. Heat transfer coefficient is weakly dependent on the plate conductivity and it is kept nearly constant in time during the heating up process. This validation is fundamental step before investigating the next, more complex configurations such as the influence of rough plates on the heat transfer.

Acknowledgment

This work was supported by the Innolot Programe - Coopernik project. The authors would like to thank the Academic Supercomputing Center TASK, Gdańsk (Poland) and PL-Grid Infrastructure for providing excellent HPC resources.

References

[1] Freidman S J and Mueller A C 1951 *Proc Gen Disc on Heat Transfer, Institution of Mech Engineers* pp 138-142

[2] Duckerman N and Lior N 2006 *Advances in Heat Transver* Vol 39, pp 565-631

[3] Chupp PRE, McFadden PW and Brown TR 1969 *Evaluation of internal heat-transfer coefficients for impingement-cooled turbine airfoils*, J Aircraft, 6, pp 203-208

[4] Florschuetz, L. W., Metzger, D. E., Su, C. C., Isod a, Y. and Tseng, H. H. (1984). *Heat transfer characteristics for jet array impingement with initial cross flow*, J of Heat Transfer, 106 (1), pp 34-41.

[5] Metzger, D. E. and Bunker, R. S. (1990). *Local heat transfer in internally cooled turbine airfoil leading edge regions: Part I – Impingement Cooling without Film Coolant Extraction*, J. of Turbo Machinery, 112 (3), pp 451-458.